

Research Article

Inspired Preparation of Zinc Oxide Nanocatalyst and the Photocatalytic Activity in the Treatment of Methyl Orange Dye and Paraquat Herbicide

Ghaida H. Munshi ^{1,2}, Amal M. Ibrahim ^{2,3} and Laila M. Al-Harbi ¹

¹Chemistry Department, Faculty of Science, King Abdulaziz University, P.O. Box 80203, Jeddah 21589, Saudi Arabia

²Chemistry Department, Faculty of Science, University of Jeddah, P.O. Box 80327, Jeddah 23218, Saudi Arabia

³Physical Chemistry Department, National Research Centre, P.O. Box 12311, Cairo 12622, Egypt

Correspondence should be addressed to Laila M. Al-Harbi; lalhrbi@kau.edu.sa

Received 13 February 2018; Revised 7 April 2018; Accepted 16 April 2018; Published 5 June 2018

Academic Editor: Jinn Kong Sheu

Copyright © 2018 Ghaida H. Munshi et al. This is an open access article distributed under the Creative Commons Attribution License, which permits unrestricted use, distribution, and reproduction in any medium, provided the original work is properly cited.

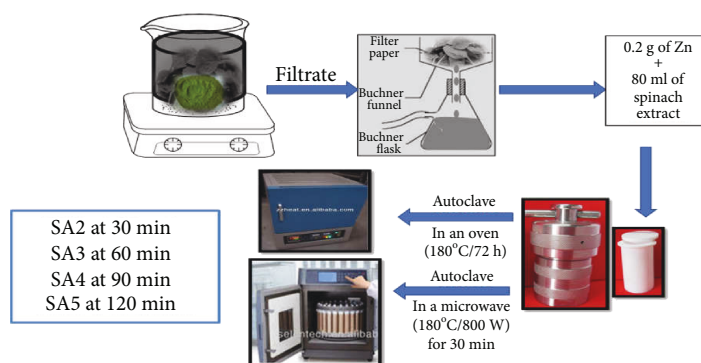
As the need to use green chemistry routes increases, environmentally friendly catalytic processes are a demand. One of the most important and abundant naturally occurring catalysts is chlorophyll. Chlorophyll is the first recognized catalyst; it is a reducing agent due to its electron-rich structure. The effects of spinach on the preparation of zinc oxide nanoparticles and the photocatalytic degradation of methyl orange and paraquat in sunlight and under a UV lamp and photocatalytic degradation in sunlight were studied. Different parameters of the catalytic preparation process and photocatalytic degradation process were studied. Characterization of differently prepared samples was carried out using different analytical techniques such as XRD, SEM, and EDX and finally the photocatalytic activity towards decomposition of methyl orange and paraquat.

1. Introduction

Nanostructure materials have attracted increasing attention during the past few decades due to their marvelous properties and a wide range of applications such as catalysis, electronics, optics, and environmental and biotechnology applications [1–6]. The increase in world demand to manipulate nanostructure materials trying to solve technological and environmental situations should be accomplished by green chemistry processes to minimize the hazards of the traditional chemical processes. Among the most widely used nanostructured metal oxides, ZnO is considered as one of the most important metal oxides with unique properties as high-surface energy, high-electron mobility, cheap, and environmentally nontoxic, and the most significant property is at wide bandgap (3.3 eV). This wide bandgap makes ZnO a field of many studies in using and improving the applications in electronics light emitters, chemical sensors, and photocatalysts [7, 8].

In general, many types of research discuss the synthesis of nanostructured materials and zinc oxide nanoparticles especially that these methods include chemical precipitation, sol-gel synthesis, hydrothermal reaction, and microwave. Many other chemical and physical attempts were carried out to improve and control the synthesis of metal oxide nanoparticles [9–12].

Green route synthesis is one of the most promising techniques for the synthesis of nanostructured materials being simple, environmentally safe (mild reaction conditions and no need for toxic chemicals) and inexpensive and can be produced in a large-scale process [13–15]. In the present work, a traditional and microwave-assisted green synthesis of ZnO using spinach extract was studied and the resulting ZnO nanoparticles were characterized using scanning electron microscopy (SEM) energy, dispersive X-ray spectroscopy (EDX), and X-ray diffraction spectroscopy (XRD); also, the catalytic activity of the obtained ZnO nanoparticles is evaluated.



SCHEME 1: Preparation equipment of ZnO catalyst both with conventional heating technique and microwave-assisted technique.

2. Materials and Methods

2.1. Materials. Zinc powder (Ranbaxy Chemicals, $>5\ \mu\text{m}$) has been used without any preheated producer or any further purification, and deionized water has been prepared in the laboratory. For the synthesis of nanomaterials, a closed cylindrical Teflon-lined stainless steel chamber of 100 ml capacity (autoclave, Latech Scientific Supply Pte. Ltd. Company) was used. 4, 4'-Bipyridine and methyl orange indicator were purchased from Sigma-Aldrich Chemical Co., and they were used without further purification.

2.2. Preparation of the Fresh Spinach Extract. Spinach (100 g) bought from a local market was washed with deionized water and patted dry with wipes. The fresh spinach leaves were heated using 200 ml of deionized water and filtered using a filter paper. The filtrate was then used to prepare zinc oxide nanoparticles.

2.3. Synthesis of Zinc Oxide Nanoparticles

2.3.1. Synthesis of Zinc Oxide Nanoparticles by Traditional Technique. Zinc metal (powder) (0.1 g) was added to 40 ml deionized (DI) water, transferred into a stainless steel Teflon-lined metallic bomb of 100 ml capacity, and sealed under inert conditions. Then, it was placed in the microwave (Milestone company (high-performance microwave digestion system) ETHOS One, SN: 1301 0243) at 800 W/180°C for 30 minutes. The furnace allowed to cool after the desired time, and the resulting suspension was centrifuged to retrieve the product (S1), washed, and then finally vacuum dried for few hours. Zinc metal (powder) (0.2 g) was added to 80 ml aqueous fresh spinach extract transferred into a stainless steel Teflon-lined metallic bomb of 100 ml capacity and sealed under inert conditions. The closed chamber was then placed in a preheated box furnace, and the mixture was heated slowly ($2^\circ\text{C}/\text{min}$) to 180°C and maintained at this temperature for 72 hours. The furnace allowed to cool after the desired time, and the resulting suspension was centrifuged to retrieve the product (SA1), washed, and then finally vacuum dried for few hours.

2.3.2. Microwave-Assisted Heating Technique. Zinc metal (0.2 gram) was added to 40 ml aqueous fresh spinach extract transferred into a stainless steel Teflon-lined metallic bomb

of 100 ml capacity and sealed under inert conditions. Then, it was placed in the microwave (Milestone company (high-performance microwave digestion system) ETHOS One, SN: 1301 0243) at 800 W/180°C for 30 minutes (SA2), 60 minutes (SA3), 90 minutes (SA4), and 120 minutes (SA5). The furnace was allowed to cool after the desired time, and the resulting suspension was centrifuged to retrieve the product, washed, and then finally vacuum dried for few hours Scheme 1.

2.4. The Photocatalytic Degradation of the Methyl Orange (MO). The photocatalytic degradation of methyl orange (MO) was performed in a Pyrex beaker using as-synthesized ZnO nanoparticles as a photocatalyst under UV illumination for various time intervals and sunlight at 48°C . MO dye (10 ppm) solution was prepared in 100 ml DI water and mixed with 0.3 g of different kinds of synthesized ZnO, in which nanoparticles powder was added to it. The resulting suspension was equilibrated by stirring for 30 min to stabilize the absorption of MO dye over the surface of the photocatalyst, that is, ZnO nanoparticles, before exposing to the light. The photocatalytic decomposition of MO was examined by measuring the absorbance at regular time intervals by using the ultraviolet and visible (UV-Vis) spectrophotometer wavelength at 465 nm. Analytical samples were taken from the reaction suspension at regular time intervals for 10 minutes and were then analyzed for their absorption using UV-Vis spectrophotometer.

2.5. The Photocatalytic Degradation of the Herbicide "Paraquat." Photocatalytic degradation experiments were carried in a reactor system that has been already described. It has a Pyrex glass tube reactor (200 ml) that can be irradiated with sunlight at 48°C temperature. Since the concentration of organic pollutants is a very important parameter in the wastewater treatment processes, we have studied the effect of paraquat initial concentration on the reaction rate to develop a kinetic model for the photocatalytic degradation of paraquat. Several experiments were carried out with paraquat aqueous solutions with different initial concentration (10 and 50–100 ppm), and different kinds of synthesized ZnO nanoparticles powder was added to it. For each of the experiments, 100 ml of a paraquat solution was placed inside the glass reactor and mixed with 0.3 g of ZnO. This slurry was

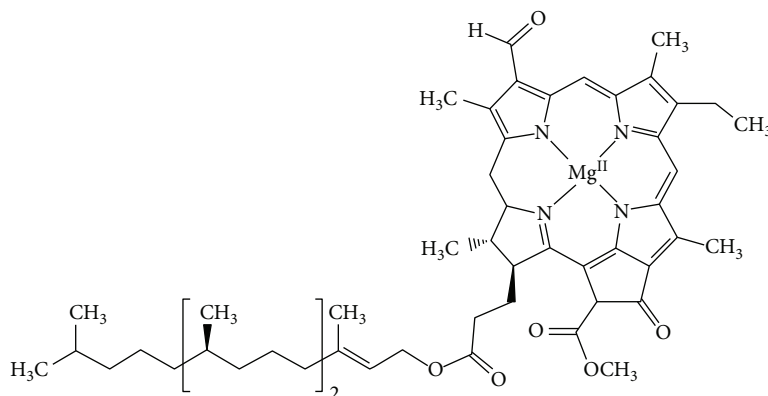
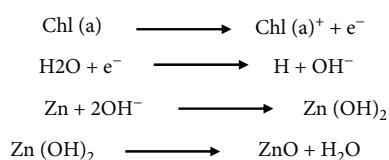


FIGURE 1: Chlorophyll a (Chl a).



SCHEME 2: A mechanism proposed for the catalytic preparation of ZnO catalyst.

agitated with a magnetic stirrer. Samples for analysis were taken at different times to monitor the reaction. Analytical samples were taken from the reaction suspension at regular time intervals for 60 min and measuring the absorbance at regular time intervals by using the UV-Vis spectrophotometer wavelength at 230 nm wavelength [16, 17].

3. Results and Discussion

Spinach is considered as an amazing green chemistry candidate, which indeed contains chlorophyll. Chlorophyll is considered as the most important naturally occurring photocatalyst on earth. The supposed mechanism of the preparation of zinc oxide could be started with the reducing effect of chlorophyll a (Chl a) (Figure 1), which can lose an electron from its aromatic π -electron system of porphyrin [18]. The reducing properties of Chl a and the produced electrons from its aromatic π -electron attack the water molecule to produce hydroxyl group (OH^-) which can attack the zinc metal to give zinc hydroxide which is eventually converted into zinc oxide (ZnO) (Scheme 2) [19].

3.1. Scanning Electron Microscope Spectroscopy (SEM). The SEM images were shown in Figure 2, representing differently prepared samples with and without the presence of spinach extract using the microwave-assisted technique as well as the conventional method. It was observed that the presence of spinach extract affected the morphology of the produced ZnO nanoparticles. Sample S1 represents the blank sample without the presence of spinach extract showing nonhomogeneous morphology with a short nanorod shape. Meanwhile, SA1 is representing ZnO nanoparticles produced in the

presence of spinach extract using the traditional technique. The image showed the homogeneous morphology of an elongated rod shape with an average diameter of 150 nm. This well-crystalline morphology could be attributed to a long time of the experiment. On the other hand, samples SA2, SA3, SA4, and SA5 represent the morphology of ZnO nanoparticles produced from the microwave-assisted technique in the presence of spinach extract for 30, 60, 90, and 120 minutes, respectively. Sample SA2 images showed low crystallinity due to the fast preparation process. As the preparation time increases, the crystallinity of the produced ZnO nanoparticles increases. The images of samples SA3, SA4, and SA5 showed agglomerated particles from smaller flower-like shape particles with an average size ranging from 50 nm to 100 nm. Energy dispersive X-ray spectrophotometry (EDX) results (Figure 3) accompanied by SEM showed that the produced nanoparticles are composed of Zn and O with Zn : O ratio in agreement.

3.2. X-Ray Diffraction Spectroscopy (XRD) of ZnO Nanoparticles. Study of standard data JCPDS 76-0704 confirmed that the synthesized materials are hexagonal ZnO phase (wurtzite structure). The pattern was indexed with hexagonal unit cell structure with P63mc, and the lattice parameters are given in Table 1. No diffraction peaks arising from any impurity can be detected in the pattern which confirms that they are the grown products of pure ZnO. The deviation of the lattice parameters is caused due to the presence of various point defects such as zinc antisites, oxygen vacancies, and extended defects, such as threading dislocation. ZnO prefers (002) direction for growth; this is attributed to the fact that the (002) plan has the lowest surface free energy [5, 20]. Both temperature and time affect the migration of atoms toward the preferred orientation. The behavior observed in XRD pattern could be attributed to the rate of heating which is considered much slower in conventional method than that in microwave-assisted technique that gives the needed time for the atoms to get their preferred orientation. The crystallite size of the produced nanoparticles was calculated by using the Scherrer formula [21].

$$D = \frac{0.9 \lambda}{\beta \cos \theta} \quad (1)$$

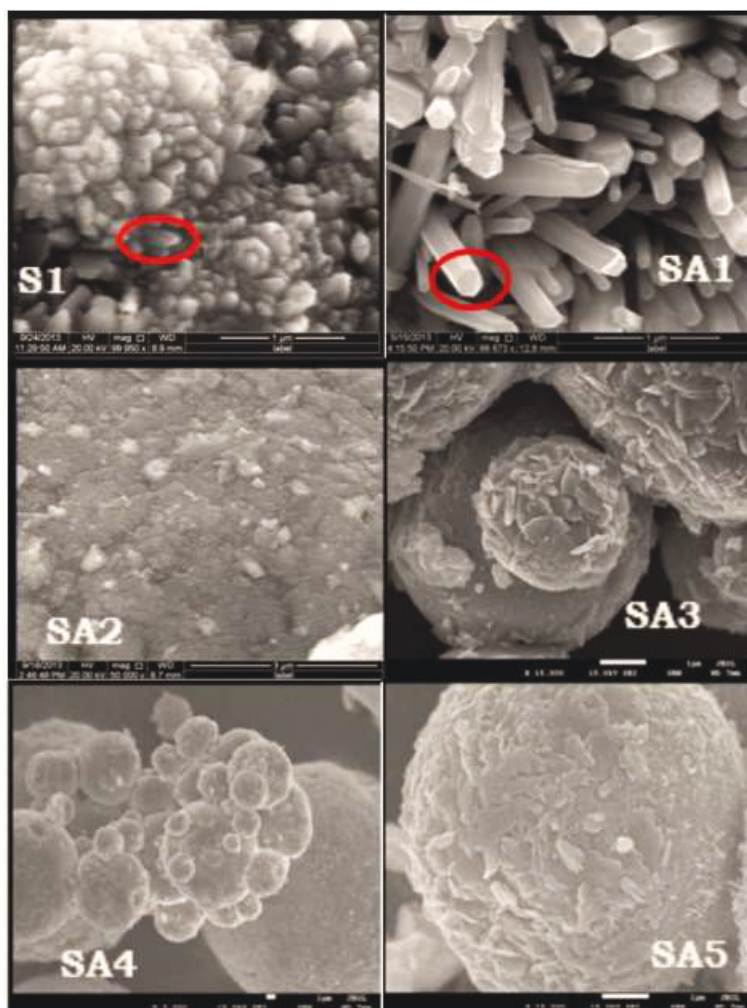


FIGURE 2: Scanning electron microscope spectroscopy images (S1: zero sample, SA1: conventional heating; SA2, SA3, SA4, and SA5 samples with assisted microwave technique).

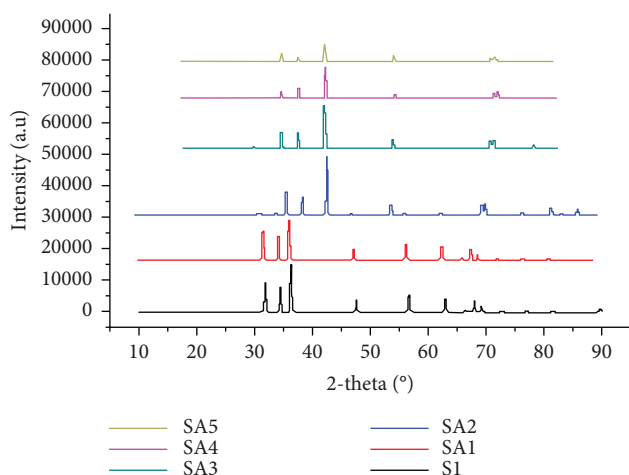


FIGURE 3: XRD patterns of ZnO nanoparticles.

where λ is the wavelength of the X-ray (0.1541 \AA), the FWHM (full width at half maximum) of the more intense peak, and the diffraction angle, and D is the particle diameter size.

3.3. Application of Catalytic Activity

3.3.1. The Photocatalytic Degradation of the Methyl Orange (MO)

(1) *Effect of Catalyst Loading under Sunlight.* A series of experiments was carried out to assess the optimum catalyst loading by varying the amount of catalyst from 0.1 g to 0.35 g of which the dye solution was prepared. The percentages of photodegradation under sunlight in 48°C with ZnO were illustrated in Figure 4. It was found that all microwave samples give almost the same percentage removal at a certain concentration, so we will discuss here only SA1. It was observed that with increasing the catalyst amount, the photodegradation increases. However, when the amount of catalyst exceeds the optimum amount (0.3 g), the photodegradation efficiency decreases. This could be attributed to the fact that

TABLE 1: The variation of lattice parameters with a variation of experimental conditions.

Sample	Volume (\AA^3)	a (\AA)	b (\AA)	c (\AA)	c/a (\AA)	Crystalline size (\AA)
S1	47.65	3.2494 (14)	3.2494 (14)	5.211 (3)	1.4914	270 (8)
SA1	47.68	3.2500 (5)	3.2500 (5)	5.2056 (9)	1.6017	488 (12)
SA2	47.73	3.2517 (9)	3.2517 (9)	5.2125 (18)	1.6030	221.1 (7)
SA3	47.63	3.2494 (17)	3.2494 (17)	5.208 (3)	1.6028	224.97 (6)
SA4	47.51	3.2473 (14)	3.2473 (14)	5.202 (2)	1.6020	600 (7)
SA5	47.57	3.2481 (14)	3.2481 (14)	5.207 (2)	1.6030	234 (2)

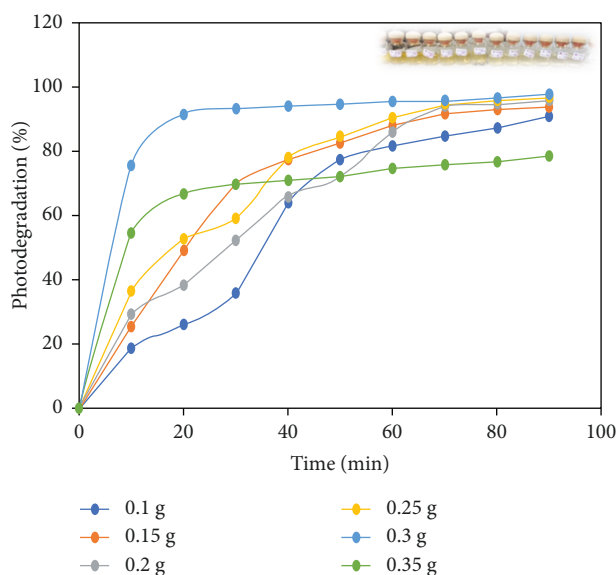


FIGURE 4: Variation of % of photodegradation versus time interval for the photodegradation of MO with a different dosage.

the number of active sites increased as the amount of the catalyst increased, till to a certain point after which the higher concentrations of the catalyst increase the turbidity of the MO suspension and the penetration of sunlight, and UV light decreases thereby increasing the scattering effect and lowering the photodegradation rate.

(2) *Effect of Different Prepared Method of Zinc Oxide Catalyst under Sunlight.* The effect of zinc oxide catalyst prepared by different methods on the dye degradation was performed by varying the kind of ZnO nanoparticles of SA1, SA2, and zinc oxide commercial (0.18 ml \approx 0.3 g) with constant catalyst loading (0.3 g) and 10 ppm of MO dye. It was observed that the prepared ZnO nanocatalysts were excellent candidates with the commercial ZnO catalyst with very promising activity, and the sample of ZnO obtained by using conventional heating technique was the most active one in degradation of MO dye (Figure 5). The high photocatalytic activity of SA1 sample could be explained by the fact that the slow rate of heating (accompanied with the traditional heating technique) provides the time needed for the ZnO nanoparticles to attain the preferred orientation. As it was noticed from SEM images, in this case, the elongated rod structure with

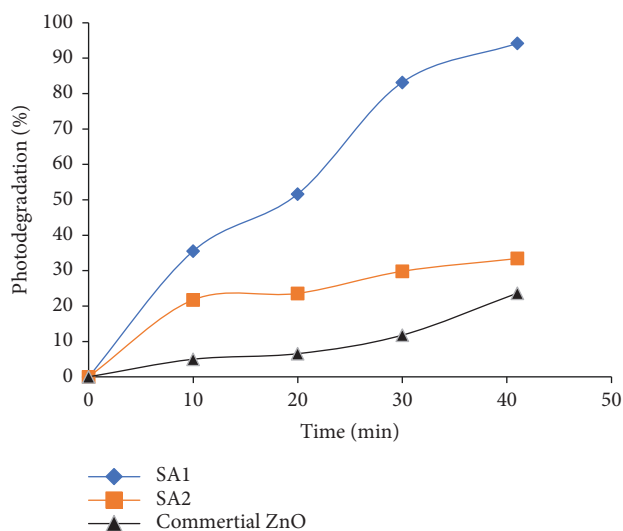


FIGURE 5: Variation of % of photodegradation versus time for various different ZnO catalyst (0.3 g) under sunlight.

small diameter increases the surface area and consequently the photocatalytic activity.

(3) *Photocatalytic Activity of Zinc Oxide Catalyst Obtained under Different Parameters under a UV Lamp.* The relationship between photodegradation efficiency of the dyes and time under UV lamp is presented in Figure 6. It is clearly observed that the sample of ZnO catalyst obtained with conventional heating technique S has 91% photodegradation efficiency to MO dye.

(4) *The Photocatalytic Degradation of the Herbicide "Paraquat".* As it was obvious from previous photocatalytic studies, step SA1 is the most active sample among the prepared ZnO photocatalyst even it gives higher activity than that of the commercial ZnO photocatalyst; thus, this study shows the photocatalytic degradation of aqueous paraquat solutions with zinc oxide (SA1) and TOC analysis illuminated under sunlight in (48°C). The ZnO sample (SA1) showed in Figure 7 features high photocatalytic activity in paraquat photodegradation. It is well known that as the concentration of the pollutant increases, the photocatalytic activity decreases due to the decrease of the tendency of the irradiating light beam to meet the catalyst particles. The paraquat

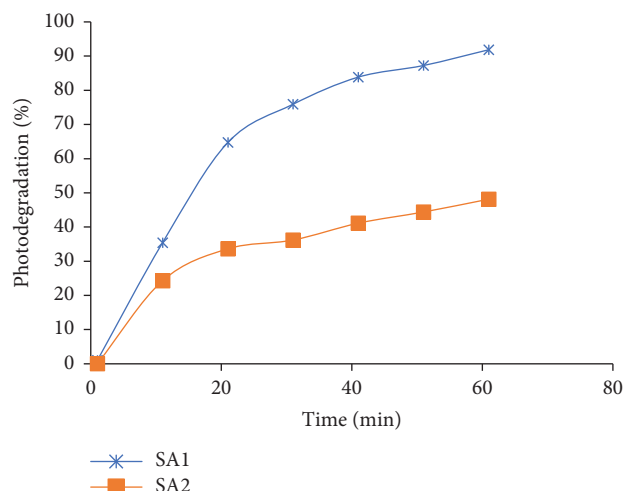


FIGURE 6: Variation of % of photodegradation versus time for various catalyst of ZnO (0.3 g) under a UV lamp.

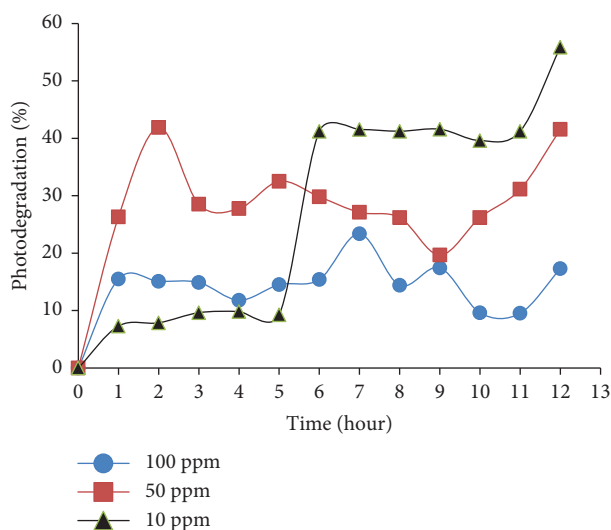


FIGURE 7: Variation of % of photodegradation versus for time of sample SA1 (0.3 g) under sunlight.

particle to catalyst particle ratio increases with increasing the concentration of paraquat. This behavior decreases the electron/hole pair formation probability, decreasing the photocatalytic activity.

(5) *Total Organic Carbon (TOC)*. TOC analysis (total organic carbon) is one of the most important monitoring tests for tracking the removal of organic pollutants from water as the TOC content in water decreases the pollutant concentration decrease. For ZnO sample (SA1), Figure 8 showed high photodegradation activity at paraquat concentration 100 ppm which leads to the decrease of TOC from 62.6 ppm to 35 ppm in 12 hours. This photodegradation activity supported the decrease in TOC with sample SA1. This behavior could be devoted to their short diameter, high crystalline, and high surface area.

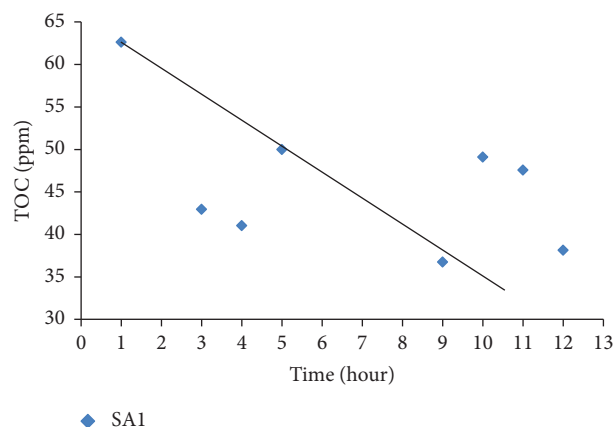


FIGURE 8: TOC values of SA1 versus time comparison photodegradation of paraquat (100 ppm) under sunlight.

4. Conclusions

The preparation of zinc oxide nanocatalyst using a green chemistry route as a catalyst (spinach extract) and also the catalytic activity evaluation of the prepared samples was studied. It is clearly concluded that the obtained ZnO nanocatalysts represent an excellent candidate with the commercial ZnO catalyst with high catalytic activity in the degradation of the methyl orange dye (MO) as well as paraquat herbicide. The produced ZnO catalyst samples were found to depend on the preparation parameters in their shape, size, and consequently catalytic activity. Among the obtained samples prepared with different heating techniques (traditional and microwave-assisted), the most promising sample is the one prepared under traditional heating technique (SA1). This behavior could be devoted to that the fact that the rate of heating in the traditional way is much slower than that in a microwave-assisted way. The slower rate of heating, in this case, provides the needed time for the produced ZnO catalyst to get the preferred crystalline orientation and in this case for the rod structure to be elongated with small diameter (150 nm); this increases the surface area and consequently increases the catalytic activity. All the used characterization and evaluation tools support the conclusion that chlorophyll is an excellent catalyst which acts under mild conditions and is favored economically.

Data Availability

The data used to support the findings of this study are available from the corresponding author upon request.

Conflicts of Interest

The authors declare that they have no conflicts of interest.

Acknowledgments

This work was funded by the King Abdulaziz City for Science and Technology (KACST), under Grant no. 177-34. The

authors, therefore, acknowledge with thanks the KASCT for technical and financial support.

References

- [1] L. L. Welbes and A. S. Borovik, "Confinement of metal complexes within porous hosts: development of functional materials for gas binding and catalysis," *Accounts of Chemical Research*, vol. 38, no. 10, pp. 765–774, 2005.
- [2] X. Wang, J. Zhou, J. Song, J. Liu, N. Xu, and Z. L. Wang, "Piezoelectric field effect transistor and nanoforce sensor based on a single ZnO nanowire," *Nano Letters*, vol. 6, no. 12, pp. 2768–2772, 2006.
- [3] M. Law, L. E. Greene, J. C. Johnson, R. Saykally, and P. Yang, "Nanowire dye-sensitized solar cells," *Nature Materials*, vol. 4, no. 6, pp. 455–459, 2005.
- [4] J. H. Lim, C. K. Kang, K. K. Kim, I. K. Park, D. K. Hwang, and S. J. Park, "UV electroluminescence emission from ZnO light-emitting diodes grown by high-temperature radiofrequency sputtering," *Advanced Materials*, vol. 18, no. 20, pp. 2720–2724, 2006.
- [5] K. Ikegami, T. Yoshiyama, K. Maejima, H. Shibata, H. Tampo, and S. Niki, "Optical dielectric constant inhomogeneity along the growth axis in ZnO-based transparent electrodes deposited on glass substrates," *Journal of Applied Physics*, vol. 105, no. 9, article 093713, 2009.
- [6] J. Schrier, D. O. Demchenko, Lin-Wang, and A. P. Alivisatos, "Optical properties of ZnO/ZnS and ZnO/ZnTe heterostructures for photovoltaic applications," *Nano Letters*, vol. 7, no. 8, pp. 2377–2382, 2007.
- [7] A. B. Djurišić, X. Chen, Y. H. Leung, and A. Man Ching Ng, "ZnO nanostructures: growth, properties and applications," *Journal of Materials Chemistry*, vol. 22, no. 14, pp. 6526–6535, 2012.
- [8] J. Bao, M. A. Zimmler, F. Capasso, X. Wang, and Z. F. Ren, "Broadband ZnO single-nanowire light-emitting diode," *Nano Letters*, vol. 6, no. 8, pp. 1719–1722, 2006.
- [9] V. Sharma, "Sol-gel mediated facile synthesis of zinc-oxide nanoaggregates, their characterization and antibacterial activity," *IOSR Journal of Applied Chemistry*, vol. 2, no. 6, pp. 52–55, 2012.
- [10] J.-S. Huang and C.-F. Lin, "Controlled growth of zinc oxide nanorod array in aqueous solution by zinc oxide sol-gel thin film in relation to growth rate and optical property," in *2008 8th IEEE Conference on Nanotechnology*, pp. 135–138, Arlington, TX, USA, August 2008.
- [11] L. M. AL-Harbi, E. H. El-Mossalamy, H. M. Arafa, A. Al-Owais, and M. A. Shah, "Growth of zinc oxide (ZnO) nanorods and their optical properties," *Modern Applied Science*, vol. 5, no. 2, 2011.
- [12] A. M. Ibrahim, M. M. Abd El-Latif, and M. S. Gohr, "Water / alcohol mediated preparation of ZnO hollow sphere," *Egyptian Journal of Chemistry*, vol. 58, no. 4, pp. 475–484, 2015.
- [13] H. Zhang, X. Ma, J. Xu, J. Niu, and D. Yang, "Arrays of ZnO nanowires fabricated by a simple chemical solution route," *Nanotechnology*, vol. 14, no. 4, pp. 423–426, 2003.
- [14] J. V. D. S. Araújo, R. V. Ferreira, M. I. Yoshida, and V. M. D. Pasa, "Zinc nanowires synthesized on a large scale by a simple carbothermal process," *Solid State Sciences*, vol. 11, no. 9, pp. 1673–1679, 2009.
- [15] J. D. Rocha, A. R. Coutinho, and C. A. Luengo, "Biopitch produced from eucalyptus wood pyrolysis liquids as a renewable binder for carbon electrode manufacture," *Brazilian Journal of Chemical Engineering*, vol. 19, no. 2, pp. 127–132, 2002.
- [16] T. Fernandes, S. Soares, T. Trindade, and A. Daniel-da-Silva, "Magnetic hybrid nanosorbents for the uptake of paraquat from water," *Nanomaterials*, vol. 7, no. 3, p. 68, 2017.
- [17] M. G. Sorolla II, M. L. Dalida, P. Khemthong, and N. Gridanurak, "Photocatalytic degradation of paraquat using nano-sized Cu-TiO₂/SBA-15 under UV and visible light," *Journal of Environmental Sciences*, vol. 24, no. 6, pp. 1125–1132, 2012.
- [18] S. Shanmugam, J. Xu, and C. Boyer, "Utilizing the electron transfer mechanism of chlorophyll a under light for controlled radical polymerization," *Chemical Science*, vol. 6, no. 2, pp. 1341–1349, 2015.
- [19] U. Maitra, S. R. Lingampalli, and C. N. R. Rao, "Artificial photosynthesis and the splitting of water to generate hydrogen," *Current Science*, vol. 106, no. 4, pp. 518–527, 2014.
- [20] Y. Sun, D. J. Riley, and M. N. R. Ashfold, "Mechanism of ZnO nanotube growth by hydrothermal methods on ZnO film-coated Si substrates," *The Journal of Physical Chemistry B*, vol. 110, no. 31, pp. 15186–15192, 2006.
- [21] B. D. Cullity, *Elements of X-Ray Diffraction*, Addison-Wesley, 2001.

